

Large-Scale Piezoelectric-Based Aircraft Systems

Subjects: Engineering, Electrical & Electronic

Contributor: Holden Li

A new approach in the development of aircraft and aerospace industry is geared toward increasing use of electric systems. An electromechanical (EM) piezoelectric-based system is one of the potential technologies that can produce a compactable system with a fast response and a high power density. However, piezoelectric materials generate a small strain, of around 0.1–0.2% of the original actuator length, limiting their potential in large-scale applications.

Keywords: piezoelectric stack ; amplification mechanism ; quasi-static stepped system ; ultrasonic system ; piezoelectric-hydraulic ; aerospace applications

1. Introduction

A concept of more/all-electric aircraft has recently received huge attention in the research and development work in the field of aerospace engineering ^{[1][2][3][4][5][6][7]}. The intent is to use more electrical systems in aircraft and aerospace applications to bring an impact on the environment ^[8]. With the fast development of electrification, more researchers and manufacturers are shifting to this dynamic trend involving a high demand for increasing the load, improving fuel efficiency, reducing emissions, and lowering the total cost of operation. Researchers seek different approaches and technologies to broaden this fashionable concept in a wide range of applications. The choice of actuators in the aircraft is based on various critical factors, such as power density, reliability, efficiency, control features, and thermal robustness, as well as the weight, size, and maintenance cost. In a commercial aircraft, actuators are essential in various applications, such as flight control, engine starter, landing system, brake actuation, and fuel pump ^{[9][10]}. The specifications of actuators in an aircraft vary across a wide range. Typical requirements can be listed as 1–320 of force, 10–700 of stroke, and 10–500 of speed, with the requirement of both modulated and two-position control methods ^[11]. For these actuation systems in the aircraft engine, the working temperature is from –50 to 150 °C at the engine intake; and it is higher for the actuators located toward the high-pressure compressor void (300–400 °C) or the tail cone area (500–600 °C) ^[12]. Overall, actuators in an aircraft require both the advantages of materials that allow them to deliver the required power in extreme environmental conditions and the optimal structural designs to maximize their performance within a constrained weight and space.

In the development of signal-by-wire and power-by-wire actuators in aircraft, electromechanical (EM) systems have seen a huge improvement, with significant results from both researchers and manufacturers. Electrical actuators, which have taken advantage of state-of-the-art motors and power screws, are among these systems ^{[13][14][15][16][17]}. The electrical actuators could provide a load range of up to 90 , with over 90% efficiency, making them suitable for replacing several conventional hydraulic or fuel-draulic systems in the jet engine ^{[18][19]}. These systems bring more advantages in terms of a compact design (eliminating pipes and heavy elements) and power-to-weight ratio (weight reducing), enhancing aircraft stability and thus providing the ability to incorporate more functions within the control system to further enhance aircraft utility. Besides electrical actuators, smart-material-based actuators are also considered a promising approach. The development of smart materials, such as piezoelectric materials ^[20], shape memory alloys ^[21], magnetostrictive materials ^[22], and electroactive polymers ^{[23][24]}, also offers advantages in the aerospace applications ^{[25][26]}. Looking beyond the potential of replacing the conventional system with similar or even better performance actuators, the smart behavior of such materials may offer more room for the development of novel systems. For example, the shape-changing ability of smart materials can be explored in morphing aircraft ^{[27][28]}. Shape memory alloy-based ^{[29][30]} and piezoelectric-based bender designs ^[31] can be used for noise reduction when mounting the bender on the trailing edge of the jet engine fan nozzle and the rotor of the helicopter, respectively. Each material responds differently to the stimuli, and various actuation modes can be achieved with distinct working concepts and geometrical designs. Among them, piezoelectric materials have shown great potential in aircraft and spacecraft applications ^{[32][33][34][35][36]}. The definition of piezoelectric materials is that they can either generate an output voltage when subjected to mechanical stress or perform a dimensional change when subjected to an electric field. These phenomena are known as direct and indirect modes of operation, which can be used for generators ^[37], sensors ^[38], and actuators ^[39]. Piezoelectric materials have the advantages of high power density,

high efficiency, driving force, and displacement resolution over electromagnetic materials. They also do not generate electromagnetic noise and are nonflammable [40][41][42]. Piezoelectric materials come in different forms, such as sheet, wafer plate, stack, fiber, and composite, which makes them suitable for diverse geometrical designs. Despite a minimal strain capability, piezoelectric actuators can deliver high power outputs with high efficiency due to their ability to be cycled at very high frequencies as compared with other actuators [43] (Figure 1).

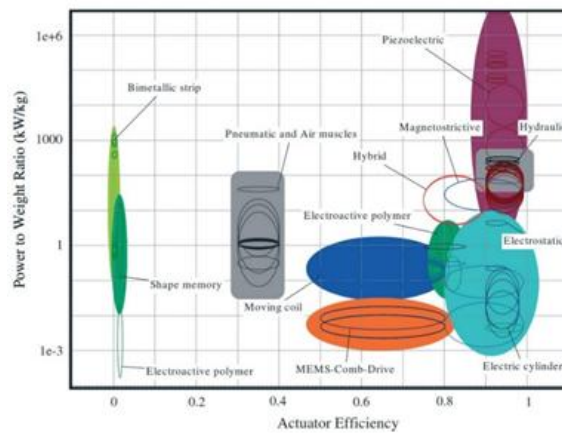


Figure 1. Power-to-weight ratio versus efficiency from a database of 220 actuators (from [43]).

Some piezoelectric materials can work in a very large temperature range, making them more promising in aircraft applications. A report from NASA revealed positive results of four piezoelectric ceramics, namely PZT-4, PZT-5A, PZT-5H, and PLZT-9/65/36, from several tests to evaluate their applicability as sensors and actuators in the intelligent aerospace system over a large temperature range, from -150 to 250 °C [44]. More efforts on material development were recorded that would gradually enhance the potential of piezoelectric materials in high-temperature industrial applications [45][46]. Therefore, piezoelectric-based systems are possible for applications located in the cold section of the aircraft engine, in which the temperature varies from -50 to 250 °C. However, amplification methods are required to generate sufficient stroke for these applications. The specifications of suitable applications for a compact piezoelectric design should be in the range of up to 5 of force, 100 of stroke, and 50 of speed. Thus the high stress and working frequency of piezoelectric actuators can be advantageous within a compact system. Some applications could be variable blow-in doors, booster bleeds, variable inlet guide vanes (IGVs), and variable stator vanes (VSVs). For instance, a piezoelectric-based linear actuator with a crank-slider mechanism was proposed to drive the IGV, which helps to control the flow that enters the jet engine and to improve the efficiency of the compressor [47][48]. Sufficient stroke of the actuator is accumulated over repeated cycles. For the same application (IGV or VSV of the gas turbine jet engine), the piezoelectric system could also be designed in such a way that a rotary motion can deliver directly to the application [49]. This actuator can be mounted on the unison ring, thus eliminating the need for other mechanical structures that add extra weight to the system. Moreover, the ability of power-off holding position of piezoelectric materials allows a design that can maintain the last controlled position in the event of failure, thus enhancing the safety level in aircraft applications.

2. Piezoelectric Actuators

2.1. Fundamentals of Piezoelectric Materials

The piezoelectric effect on ceramic materials was discovered in 1880 by Nobel laureates Pierre and Jacques Curie. A piezoelectric transducer can be used as both generator [50] and actuator [51]. Specifically, the direct piezoelectric effect is used in the generator, while the indirect piezoelectric effect is used for the actuator [52]. The direct piezoelectric effect refers to the development of electrical charges on applications of mechanical stress, and vice versa (indirect piezoelectric effect). For the actuation applications reviewed in this paper, the piezoelectric material deforms with the applied electric field to produce mechanical energy.

The most commonly used piezoelectric materials are piezoelectric ceramic, such as lead zirconate titanate (PZT), barium titanate (BaTiO_3), and lead titanate (PbTiO_3). With a polycrystalline structure, ceramic materials can be fabricated into a variety of shapes and sizes. Besides, with the effort to reduce and avoid lead (Pb) in piezoelectric materials, lead-free piezoelectric development has been gaining momentum in recent years [52][53][54][55]. Some of these materials are alkali-metal-based bismuth sodium titanate (BNT), bismuth potassium titanate (BKT) [56], and potassium sodium niobate (KNN) [57]. To increase the potential of piezoelectricity in various working conditions, high-temperature piezoelectric materials have been developed, such as $\text{Pb}(\text{NbO}_3)_2$ and $\text{Bi}_4\text{Ti}_3\text{O}_{12}$. However, the strain and stress of these materials may be reduced. In general, piezoelectric materials have a very small strain, of 0.1–0.2%, but with high stress, in the range of

100–131 MPa. Their specific power density is around 1000 kW/kg, and they have high efficiency, of more than 80% [58]. However, piezoelectric materials experience some drawbacks, such as substantial hysteresis [59], temperature-dependent properties [60], and fracture behaviors [61]. These phenomena eventually affect the performance of the piezoelectric materials, especially the stroke and accuracy of piezoelectric actuators.

The performance of the piezoelectric actuator is determined by the material properties known as the electromechanical coefficients. The most common material properties are the directional piezoelectric charge constants. The mechanical strain () of a piezoelectric material can be found by the relation

$$S = s^E T + dE \quad (1)$$

where s^E is the compliance or elasticity coefficient, T is the mechanical stress, d is the piezoelectric charge constant, and E is the electric field (, where V is the applied voltage and t is the thickness of the material).

The coupling coefficient of the piezoelectric can be divided into three groups corresponding to the orientations of the electric field and the displacement. These coefficients are d_{31} , d_{32} , and d_{33} , corresponding to three deformation modes: longitudinal, transversal (Figure 2a), and shear modes (Figure 2b), respectively. In general, the strain and electromechanical conversion efficiency are higher in the longitudinal direction [62][63]. Therefore, this deformation mode is usually used in actuators, especially in the stacked configuration. Table 1 below shows examples of some piezoelectric materials and their properties that are commonly used in the piezoelectric-based system.

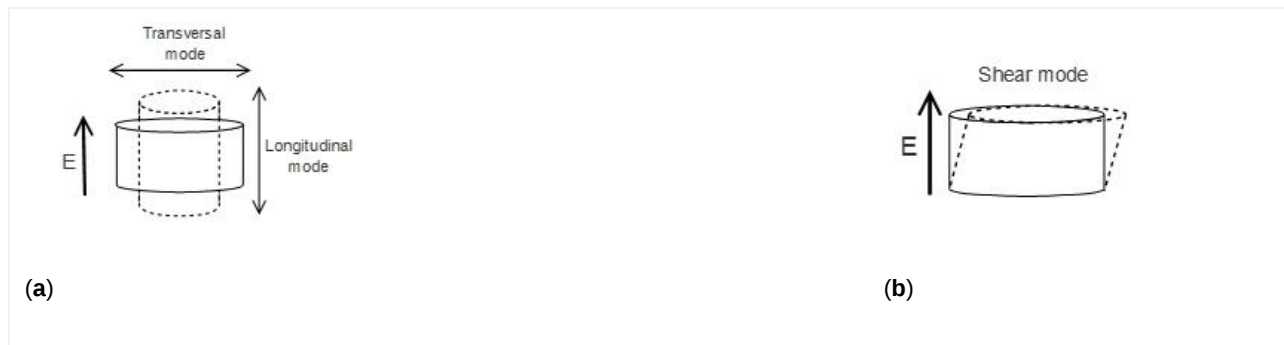


Figure 2. Deformation of the piezoelectric actuator. (a) Longitudinal and transversal mode; (b) shear mode.

Table 1. Examples of some properties of piezoelectric materials.

Materials	at Room Temp. (pC/N)	Curie Temp. T_C (°C)	Operating Temp. (°C)	Reference
PZT powder	590–610	-	-	[20]
PMN-PT	2000–3500	120–130	Up to 80	[60]
PZN-PT	1900–2000	160	Up to 110	[64]
PZT-5H	585	170	–150–125	[44]
PZT Navy Type III (Hard) ¹	<300	305	Up to 220	[45]
PZT-4	225	310	–150–100	[44]
PZT Navy Type II (Soft) ₂	<600	340	Up to 200	[45]
PZT-5A	350	350	Up to 250	[44]

PIC series	240–500	160–370	–40–150	[65]
Lead-free materials				
BTBK	58.9–117	170–223	-	[56]
BNT	91	320	-	[56]
KNN	80–160	Up to 400	-	[57]
High-temperature materials				
Pb(NbO ₃) ₂	81	550	Up to 300	[45]
Bi ₄ Ti ₃ O ₁₂	3.5	675	Up to 675	[45]
Bi ₄ Ti _{2.86} Nb _{0.14} O ₁₂	20	655	Up to 655	[45]

¹ Hard: less hysteresis loss, good stability under high mechanical loads, and operating field strength; thus good for ultrasonic transducers. ² Soft: large hysteresis loss, large piezoelectric charge coefficient, and easy polarization at low field strength; thus ideal for actuator and sensor applications.

Piezoelectric elements can come in different geometrical forms, such as thin plate, single layer, multilayer, torsion tube. Besides these designs, macro piezo fiber composite (MFC) is another form of piezoelectric that was invented by NASA back in the 1990s and has been commercialized by Smart Material since 2002 [66][67]. Constructed of piezoelectric-ceramic-based fibers (usually PZT 5A or PZT Navy Type II) sandwiched between electrodes and polyimide layers, MFCs can produce elongation, contraction, and bending motions for actuation [68]. They can also function in sensitive sensor and vibration harvesting applications [69][70]. With a flexible nature, these piezoelectric composites have greater durability and reliability and can be attached to the surface of or embedded inside the structures. They have been proposed to be used in various aerospace applications, such as aircraft health structure monitoring, noise and vibration control of helicopter rotors, and surface control of morphing wings [71]. MFCs can find more aerospace applications if high-temperature piezoelectric (see Table 1), electrode, and adhesive materials are explored [72]. Table 2 below summarizes the performance of commercial piezoelectric actuators with some typical geometrical forms.

Table 2. Typical displacement and resonant frequency of typical geometrical forms of commercial piezoelectric actuators.

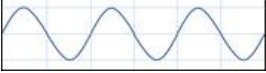


Form	Typical Size	Displacement Range	Resonant Frequency
Single layer (wafer)	A few hundred micrometer thickness	Up to 0.1	Up to 100
Multilayer extension (rectangle, round, hollow stacks)	Up to 100 area & 100 in length	Up to 100	Up to 100 and more
Multilayer shearing	Up to ~250 area & 50 length	Up to 10	Up to 100 and more
Piezo bender (unimorph/bimorph)	<1 thickness	10 to 2	Up to a few kilohertz

Macrofiber composite (elongation)	Up to 140 active length	Up to 150 ¹	From to megahertz
Macrofiber composite (contraction)	Up to 170 active length	Up to 100 ²	From to megahertz

¹ Free strain: up to 1050 ppm. ² Free strain: up to -600 ppm.

The piezoelectric actuator can be powered by a periodic voltage with sinusoidal, sawtooth, or rectangle waveforms. Depending on the required movements, each piezoelectric mechanism requires a customized input signal with a particular pattern, amplitude, and frequency to maximize its performance. In the event of more than one piezoelectric element being involved in the design, the phase difference of the controlled signal of each piezoelectric actuator needs to be designed precisely to obtain the coupling performance. The sinusoidal, square/rectangle, and sawtooth waveforms are commonly used in the stepped-motion piezoelectric system (Table 3). Power consumption during the operation of piezoelectric actuators is directly proportional to the capacitance of the device by the relation shown in Table 3.

Table 3. Typical input signals and related power consumption for piezoelectric actuators.

Sinusoidal Waveform	Square/Rectangle Waveform	Sawtooth Waveform
		
$P = \pi f C [V_{pp}]^2 / 4$	$P = f C [V_{pp}]^2$	$P = f C [V_{pp}]^2 / \sqrt{3}$

where f is the working frequency, C is the capacitance of the piezoelectric, and V_{pp} is the applied peak to peak voltage. The piezoelectric heat dissipation is usually 10% of the power supplied to the load. Therefore, the selection of usage piezoelectric materials and operating conditions must be weighed against the consumed power to ensure that the system's power budget is optimized.

2.2. Piezoelectric Stacks

Piezoelectric materials can be stacked together and be sandwiched between electrode layers to achieve a higher stroke for actuator applications [73][74]. Adopting the name of the manufacturing method, they are known as the piezoelectric stack or the multilayer piezoelectric (Figure 3). Piezoelectric stacks and piezoelectric actuators are manufactured and developed by various companies, such as Physik Instrumente (PI), Tokin Corporation, Cedrat Technologies, PiezoDrive, PiezoMotor, Piezosystem Jena, and CTS Corporation. Usually, the length of the stack is limited to 150 mm and the area is less than 225 cm². The commercial piezoelectric stack usually offers a stroke range from several micrometers to a hundred micrometers (longitudinal mode) and a blocked force range from a hundred to a few thousand N. The size and shape of a piezoelectric stack can be customized to generate the required force and stroke. In the case of large stroke applications, an amplification mechanism is preferred.

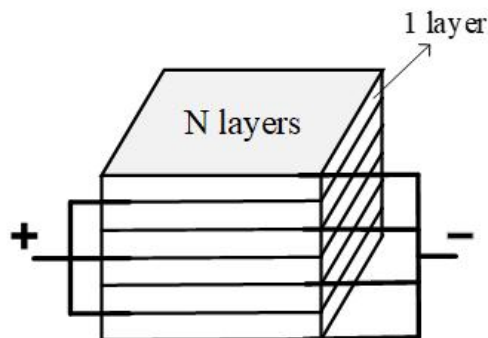


Figure 3. The electrical connection of an N -layers piezoelectric stack.

The stroke () of the stack is scaled with the number of stacking layers (Equation (2)), while the output force () is related to the active area of the piezoelectric actuators (Equation (3)).

$$\Delta L = V_p p \times d_3 3 \times N \quad (2)$$

$$F_b = V_p p \times d_3 3 \times YA/L_0 \quad (3)$$

where, is the piezoelectric constant (longitudinal mode), is the number of stacking layers, is the modulus of the piezoelectric material, is the area of each layer, and is the initial thickness of each layer. The force and stroke of the piezoelectric stack are under an electrical load (applied voltage), and the mechanical load is shown in Figure 4. When the piezoelectric stacks are implemented in a cyclic process, they will be subjected to a severe hysteresis characteristic affected by the frequency and magnitude of the applied voltage. Therefore, closed-loop control is required to compensate for the hysteresis effect in precise positioning applications [75].

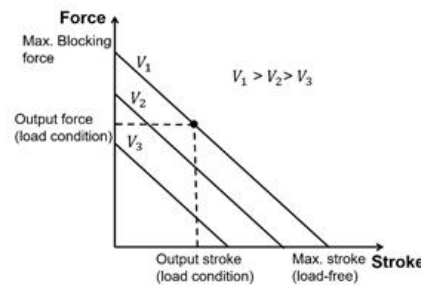


Figure 4. Force–stroke characteristic of the piezoelectric stack.

2.3. Classification of Amplification Methods

The microstroke range of a stand-alone piezoelectric stack can be further amplified to the required level using external amplifiers, such as mechanical, hydraulic, or other kinetic mechanisms, depending on the architecture. Several conceptual designs are proposed and used, such as the amplified mechanism by the compliant structure, the inchworm mechanism, the walking mechanism, and the hybrid electro-hydraulic system. In this paper, the amplification methods are divided into four groups, as shown in Figure 5. Each technique will be discussed in subsequent sections.

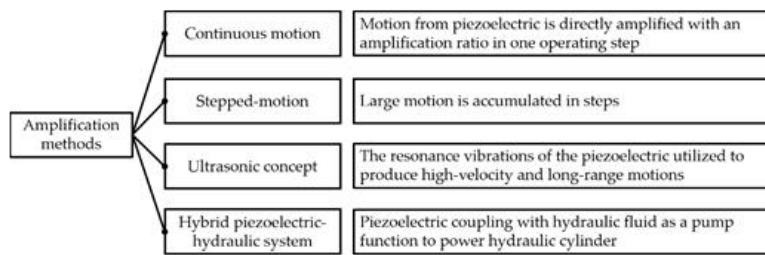


Figure 5. Summary of amplification methods.

References

1. Rubertus, D.P.; Hunter, L.D.; Cecere, G.J. Electromechanical Actuation Technology for the All-Electric Aircraft. *IEEE Trans. Aerosp. Electron. Syst.* 1984, AES-20, 243–249, doi:10.1109/TAES.1984.310506.
2. Rosero, J.A.; Ortega, J.A.; Aldabas, E.; Romeral, L. Moving towards a more electric aircraft. *IEEE. Aerosp. Electron. Syst. Mag.* 2007, 22, 3–9, doi:10.1109/MAES.2007.340500.
3. Qiao, G.; Liu, G.; Shi, Z.; Wang, Y.; Ma, S.; Lim, T.C. A review of electromechanical actuators for More/All Electric aircraft systems. *Proc. Inst. Mech. Eng. C. J. Mech. Eng. Sci.* 2017, 232, 4128–4151, doi:10.1177/0954406217749869.
4. MarÉ, J.-C.; Fu, J. Review on signal-by-wire and power-by-wire actuation for more electric aircraft. *Chin. J. Aeronaut.* 2017, 30, 857–870, doi:10.1016/j.cja.2017.03.013.
5. Viswanathan, V.; Knapp, B.M. Potential for electric aircraft. *Nat. Sustain.* 2019, 2, 88–89, doi:10.1038/s41893-019-0233-2.

6. Cecati, C.; Song, S.; Buticchi, G. Special Issue on More Electric Aircraft. *IEEE Trans. Transp. Electrification* 2020, 6, 1382–1385, doi:10.1109/TTE.2020.3026761.
7. Emmanouil, K. Reliability in the era of electrification in aviation: A systems approach. *Microelectron. Reliab.* 2020, 114, 113945, doi:10.1016/j.microrel.2020.113945.
8. Zaporozhets, O.; Isaienko, V.; Synylo, K. Trends on current and forecasted aircraft hybrid electric architectures and their impact on environment. *Energy* 2020, 211, 118814, doi:10.1016/j.energy.2020.118814.
9. Janker, P.; Claeysen, F.; Grohmann, B.; Christmann, M.; Lorkowski, T.; LeLetty, R.; Sosniki, O.; Pages, A. New actuators for aircraft and space applications. In *Proceedings of the 11th International Conference on New Actuators*, Bremen, Germany, 9–11 June 2008; pp. 325–330.
10. Todeschi, M. Airbus—EMAs for Flight Controls Actuation System—An Important Step Achieved in 2011; SAR Technical Papers; SAE International: Warrendale, PA, USA, 2011, Volume 1, doi:10.4271/2011-01-2732.
11. Jensen, S.C.; Jenney, G.D.; Dawson, D. Flight test experience with an electromechanical actuator on the F-18 Systems Research Aircraft. In *Proceedings of the 19th DASC. 19th Digital Avionics Systems Conference; Proceedings (Cat. No. 00CH37126)*, 7–13 October 2000, Philadelphia, PA, USA; Volume 311, pp. 2E3/1–2E3/10, doi:10.1109/DASC.2000.886914.
12. Newman, R. The More Electric Engine Concept. *SAE Trans.* 2004, 113, 1656–1661, doi:10.4271/2004-01-3128.
13. Bennett, J.W.; Mecrow, B.C.; Jack, A.G.; Atkinson, D.J. A Prototype Electrical Actuator for Aircraft Flaps. *IEEE Trans. Ind. Appl.* 2010, 46, 915–921, doi:10.1109/TIA.2010.2046278.
14. Cao, W.; Mecrow, B.C.; Atkinson, G.J.; Bennett, J.W.; Atkinson, D.J. Overview of Electric Motor Technologies Used for More Electric Aircraft (MEA). *IEEE Trans. Ind. Electron.* 2012, 59, 3523–3531, doi:10.1109/TIE.2011.2165453.
15. Budinger, M.; Liscouët, J.; Hospital, F.; Maré, J.C. Estimation models for the preliminary design of electromechanical actuators. *Proc. Inst. Mech. Eng. G. J. Aerosp. Eng* 2011, 226, 243–259, doi:10.1177/0954410011408941.
16. Fu, J.; Maré, J.-C.; Fu, Y. Modelling and simulation of flight control electromechanical actuators with special focus on model architecting, multidisciplinary effects and power flows. *Chin. J. Aeronaut.* 2017, 30, 47–65, doi:10.1016/j.cja.2016.07.006.
17. Giangrande, P.; Galassini, A.; Papadopoulos, S.; Al-Timimy, A.; Calzo, G.L.; Degano, M.; Galea, M.; Gerada, C. Considerations on the Development of an Electric Drive for a Secondary Flight Control Electromechanical Actuator. *IEEE Trans. Ind. Appl.* 2019, 55, 3544–3554, doi:10.1109/TIA.2019.2907231.
18. Moir, I.; Seabridge, A.G. *Aircraft Systems: Mechanical, Electrical, and Avionics Subsystems Integration*, 3rd ed.; Wiley: Chichester, UK, 2008; doi:10.1002/9780470770931.
19. Ismagilov, F.R.; Vavilov, V.E.; Sayakhov, I.F. Mathematical model of an aircraft electromechanical actuator with flex coupling. In *Proceedings of the 2017 Dynamics of Systems, Mechanisms and Machines (Dynamics)*, Omsk, Russia, 14–16 November 2017; pp. 1–5, doi:10.1109/Dynamics.2017.8239456.
20. Panda, P.K.; Sahoo, B. PZT to Lead Free Piezo Ceramics: A Review. *Ferroelectrics* 2015, 474, 128–143, doi:10.1080/0150193.2015.997146.
21. Sun, L.; Huang, W.M.; Ding, Z.; Zhao, Y.; Wang, C.C.; Purnawali, H.; Tang, C. Stimulus-responsive shape memory materials: A review. *Mater. Des.* 2012, 33, 577–640, doi:10.1016/j.matdes.2011.04.065.
22. Apicella, V.; Clemente, C.S.; Davino, D.; Leone, D.; Visone, C. Review of Modeling and Control of Magnetostrictive Actuators. *Actuators* 2019, 8, 45, doi:10.3390/act8020045.
23. Bar-Cohen, Y. Electroactive polymers as artificial muscles—Reality and challenges. In *Proceedings of the 19th AIAA Applied Aerodynamics Conference*, Anaheim, CA, United States, 11–14 June 2001; p. 1492, doi:10.2514/6.2001-1492.
24. Bashir, M.; Rajendran, P. A review on electroactive polymers development for aerospace applications. *J. Intell. Mater. Syst. Struct.* 2018, 29, 3681–3695, doi:10.1177/1045389X18798951.
25. Crawley, E.F. Intelligent structures for aerospace—A technology overview and assessment. *AIAA J.* 1994, 32, 1689–1699, doi:10.2514/3.12161.
26. Basheer, A.A. Advances in the smart materials applications in the aerospace industries. *Aircr. Eng. Aerosp. Technol.* 2020, 92, doi:10.1108/AEAT-02-2020-0040.
27. Sun, J.; Guan, Q.; Liu, Y.; Leng, J. Morphing aircraft based on smart materials and structures: A state-of-the-art review. *J. Intell. Mater. Syst. Struct.* 2016, 27, 2289–2312, doi:10.1177/1045389X16629569.
28. Grohmann, B.; Maucher, C.; Jänker, P. Actuation concepts for morphing helicopter rotor blades. In *Proceedings of the 25th International Congress of the Aeronautical Sciences*, Hamburg, Germany, 3–8 September 2006.

29. Calkins, F.; Butler, G.; Mabe, J. Variable Geometry Chevrons for Jet Noise Reduction. In Proceedings of the 12th AIAA/CEAS Aeroacoustics Conference (27th AIAA Aeroacoustics Conference), Cambridge, MA, USA, 8–10 May 2006, doi:10.2514/6.2006-2546.
30. Calkins, F.T.; Mabe, J.H. Shape Memory Alloy Based Morphing Aerostructures. *J. Mech. Des.* 2010, 132, doi:10.1115/1.4001119.
31. Jaenker, P.; Kloeppel, V.; Konstanzer, P.; Maier, R. Piezo active vibration and noise control in helicopters. In Proceedings of the 26th Congress of International Council of the Aeronautical Sciences, Anchorage, AK, USA, 14–19 September 2008; pp. 1–10.
32. Loewy, R.G. Recent developments in smart structures with aeronautical applications. *Smart Mater. Struct.* 1997, 6, R11–R42, doi:10.1088/0964-1726/6/5/001.
33. Philippe, B.; Frank, C.; Ronan Le, L. Amplified piezoelectric actuators: From aerospace to underwater applications. In Proceedings of the SPIE 5388, Smart Structures and Materials 2004: Industrial and Commercial Applications of Smart Structures Technologies, San Diego, CA, USA, 29 July 2004, doi:10.1117/12.540781.
34. Sherit, S. Smart material/actuator needs in extreme environments in space. In Proceedings of the SPIE 5761, Smart Structures and Materials 2005: Active Materials: Behavior and Mechanics, San Diego, CA, USA, 16 May 2005, doi:10.1117/12.606475.
35. Uchino, K. Piezoelectric actuators 2006. *J. Electroceramics* 2008, 20, 301–311, doi:10.1007/s10832-007-9196-1.
36. Elahi, H.; Munir, K.; Eugeni, M.; Abrar, M.; Khan, A.; Arshad, A.; Gaudenzi, P. A Review on Applications of Piezoelectric Materials in Aerospace Industry. *Integr. Ferroelectr.* 2020, 211, 25–44, doi:10.1080/10584587.2020.1803672.
37. Lagomarsini, C.; Jean-Mistral, C.; Lombardi, G.; Sylvestre, A. Hybrid piezoelectric–electrostatic generators for wearable energy harvesting applications. *Smart Mater. Struct.* 2019, 28, 035003, doi:10.1088/1361-665X/aaf34e.
38. Jiao, P.; Egbe, K.-J.I.; Xie, Y.; Matin Nazar, A.; Alavi, A.H. Piezoelectric Sensing Techniques in Structural Health Monitoring: A State-of-the-Art Review. *Sensors* 2020, 20, doi:10.3390/s20133730.
39. Wang, S.; Rong, W.; Wang, L.; Xie, H.; Sun, L.; Mills, J.K. A survey of piezoelectric actuators with long working stroke in recent years: Classifications, principles, connections and distinctions. *Mech Syst Signal. Process.* 2019, 123, 591–605, doi:10.1016/j.ymssp.2019.01.033.
40. Huber, J.; Fleck, N.; Ashby, M. The selection of mechanical actuators based on performance indices. *Proc. Math. Phys. Eng. Sci.* 1997, 453, 2185–2205, doi:10.1098/rspa.1997.0117.
41. Xiaoning, J.; Paul, W.R.; Wesley, S.H.; Edward, S.; Shuxiang, D.; Dwight, V.; Jim, M., Jr.; Brian, P. Advanced piezoelectric single crystal based actuators. In Proceedings of the SPIE 5761, Smart Structures and Materials 2005: Active Materials: Behavior and Mechanics, San Diego, CA, USA, 16 May 2005, doi:10.1117/12.600019.
42. Dong, S. Review on piezoelectric, ultrasonic, and magnetoelectric actuators. *J. Adv. Dielectr* 2012, 02, 1230001, doi:10.1142/S2010135X12300010.
43. Zupan, M.; Ashby, M.F.; Fleck, N.A. Actuator Classification and Selection—The Development of a Database. *Adv. Eng. Mater.* 2002, 4, 933–940, doi:10.1002/adem.200290009.
44. Hooker, M.W. Properties of PZT-based Piezoelectric Ceramics Between -150 and 250 C; NASA/CR-1998-208708; Langley Research Center: Hampton, VA, USA, 1998.
45. Stevenson, T.; Martin, D.G.; Cowin, P.I.; Blumfield, A.; Bell, A.J.; Comyn, T.P.; Weaver, P.M. Piezoelectric materials for high temperature transducers and actuators. *J. Mater. Sci. Mater. Electron.* 2015, 26, 9256–9267, doi:10.1007/s10854-015-3629-4.
46. Huang, S.; Zeng, J.; Zheng, L.; Man, Z.; Ruan, X.; Shi, X.; Li, G. A novel piezoelectric ceramic with high Curie temperature and high piezoelectric coefficient. *Ceram. Int.* 2020, 46, 6212–6216, doi:10.1016/j.ceramint.2019.11.089.
47. Rusovici, R.; Choon, S.T.-C.K.; Sepri, P.; Feys, J. Smart actuation of inlet guide vanes for small turbine engine. In Proceedings of the SPIE 7981, Sensors and Smart Structures Technologies for Civil, Mechanical, and Aerospace Systems 2011, San Diego, CA, USA, 15 April 2011; p. 79813F, doi:10.1117/12.881953.
48. Rusovici, R. Apparatus and Method for Rotating Fluid Controlling Vanes in Small Turbine Engines and Other Applications. U.S. Patent US9394804B2, 19 July 2016.
49. Vonfelt, J.-J.C.; Klonowski, T.; Moutaux, A. A Device for Controlling Inlet Guide Vanes by Means of a Multilayer Piezoelectric Actuator. U.S. Patent US10731504B2, 4 August 2020.
50. Erturk, A.; Inman, D.J. Piezoelectric Energy Harvesting; John Wiley & Sons: Chichester, UK, 2011; pp. 412.
51. Craig, D.N. Piezoelectric actuator technology. In Proceedings of the SPIE 2717, Smart Structures and Materials 1996: Smart Structures and Integrated Systems, San Diego, CA, USA, 1 May 1996, doi:10.1117/12.239027.

52. Shafik, A.; Ben Mrad, R. Piezoelectric Motor Technology: A Review. In *Nanopositioning Technologies: Fundamentals and Applications*, Ru, C., Liu, X., Sun, Y., Eds. Springer: Cham, Switzerland, 2016; pp. 33–59, doi:10.1007/978-3-319-23853-1_2.
53. Saito, Y.; Takao, H.; Tani, T.; Nonoyama, T.; Takatori, K.; Homma, T.; Nagaya, T.; Nakamura, M. Lead-free piezoceramics. *Nature* 2004, 432, 84–87, doi:10.1038/nature03028.
54. Shrout, T.R.; Zhang, S.J. Lead-free piezoelectric ceramics: Alternatives for PZT? *J. Electroceramics* 2007, 19, 113–126, doi:10.1007/s10832-007-9047-0.
55. Khesro, A.; Wang, D.; Hussain, F.; Sinclair, D.C.; Feteira, A.; Reaney, I.M. Temperature stable and fatigue resistant lead-free ceramics for actuators. *Appl. Phys. Lett.* 2016, 109, 142907, doi:10.1063/1.4964411.
56. Takenaka, T.; Nagata, H. Current status and prospects of lead-free piezoelectric ceramics. *J. Eur. Ceram. Soc.* 2005, 25, 2693–2700, doi:10.1016/j.jeurceramsoc.2005.03.125.
57. Ringgaard, E.; Wurlitzer, T.; Wolny, W.W. Properties of Lead-Free Piezoceramics Based on Alkali Niobates. *Ferroelectrics* 2005, 319, 97–107, doi:10.1080/00150190590965497.
58. Poole, A.; Booker, J.D. Classification and selection of actuator technologies with consideration of stimuli generation. In *Proceedings of the SPIE 6927, Electroactive Polymer Actuators and Devices (EAPAD) 2008*, San Diego, CA, USA, 10 April 2008; p. 692728, doi:10.1117/12.775426.
59. Hassani, V.; Tjahjowidodo, T. A hysteresis model for a stacked-type piezoelectric actuator. *Mech. Adv. Mater. Struct.* 2017, 24, 73–87, doi:10.1080/15376494.2015.1107668.
60. Benayad, A.; Sebald, G.; Guiffard, B.; Lebrun, L.; Guyomar, D.; Pleska, E. Temperature dependence of piezoelectric properties of PMN-PT and PZN-PT single crystals. *J. Phys. IV France* 2005, 126, 53–57, doi:10.1051/jp4:2005126011.
61. Suo, Z.; Kuo, C.M.; Barnett, D.M.; Willis, J.R. Fracture mechanics for piezoelectric ceramics. *J. Mech. Phys. Solid* 1992, 40, 739–765, doi:10.1016/0022-5096(92)90002-J.
62. Yano, T.; Takahashi, S. Utilization of piezoelectric stiffened effects on impact printer heads. *Electron. Commun. Jpn. Part II Electron.* 1989, 72, 19–32, doi:10.1002/ecjb.4420721003.
63. Hollerbach, J.M.; Hunter, I.W.; Ballantyne, J. A comparative analysis of actuator technologies for robotics. In *The Robotics Review 2*, Khatib, O., Craig, J.J., Lozano-Perez, T., Eds. MIT Press: Cambridge, MA, USA, 1991; Volume 2, pp. 299–342.
64. Hana, P.; Burianova, L.; Furman, E.; Cross, L.E. Dielectric Properties of PZN-PT Single Crystals Influenced by Electric Field in a Wide Temperature Range. *Ferroelectrics* 2003, 293, 321–330, doi:10.1080/00150190390238702.
65. Piezoelectric Materials. Available online: <https://www.physikinstrumente.com/en/technology/piezo-technology/piezoelectric-materials/#c15163> (accessed on 28 July 2020).
66. Wilkie, W.; High, J.; Bockman, J. Reliability testing of NASA Piezocomposite Actuators. 2002. Available online: <https://ntrs.nasa.gov/citations/20030014135> (accessed on 15 January 2021).
67. Wilkie, W. NASA MFC piezocomposites: A development history. In *Proceedings of the International Symposium on Macro Fiber Composite Applications ISMA, Volkswagen “Transparent Factory”*, Dresden, Germany, 27–28 September 2005.
68. Macro Fiber Composite Actuator & Sensor. Available online: <https://www.smart-material.com/MFC-product-main.html> (accessed on 12 January 2020).
69. Andreas, J.S.; Thomas, D.; Bent, B.; Christian, F.; Ludwig, H.; Thomas, R. Overview on macrofiber composite applications. In *Proceedings of the SPIE 6170, Smart Structures and Materials 2006: Active Materials: Behavior and Mechanics*, San Diego, CA, USA, 6 April 2006, doi:10.1117/12.658914.
70. Macro Fiber Composite Generators. Available online: <https://www.smart-material.com/EH-MFC-generators.html> (accessed on 12 January 2020).
71. Thomas, P.R.; Blázquez Calzada, Á.C.; Gilmour, K. Modeling of macro fiber composite actuated laminate plates and aero-foils. *J. Intell. Mater. Syst. Struct.* 2019, 31, 525–549, doi:10.1177/1045389X19888728.
72. Lee, H.J.; Zhang, S.; Bar-Cohen, Y.; Sherit, S. High Temperature, High Power Piezoelectric Composite Transducers. *Sensors* 2014, 14, 14526–14552, doi:10.3390/s140814526.
73. Anderson, E.; Moore, D.; Fanson, J.; Ealey, M. Development of an active member using piezoelectric and electrostrictive actuation for control of precision structures. In *Proceedings of the 31st Structures, Structural Dynamics and Materials Conference*, Long Beach, CA, USA, 2–4 April 1990, doi:10.2514/6.1990-1085.
74. Straub, F.K.; Merkley, D.J. Design of a smart material actuator for rotor control. *Smart Mater. Struct.* 1997, 6, 223–234, doi:10.1088/0964-1726/6/3/002.

75. Ru, C.; Sun, L. Improving positioning accuracy of piezoelectric actuators by feedforward hysteresis compensation based on a new mathematical model. *Rev. Sci. Instrum.* 2005, 76, 095111, doi:10.1063/1.2052047.
-

Retrieved from <https://encyclopedia.pub/entry/history/show/17448>